ISSN No: 2348-4845
International Journal & Magazine of Engineering, Technology, Management and Research
A Peer Reviewed Open Access International Journal

10-MWwind generation with the Large Permanent Magnet Wind Generator Systems by using Fuzzy Logic controller

Mr.Ponnam Prasanna Kumar
PG Scholar,
Department of EEE,
E.V.M College of Engineering and Technology.

Mr.Mahesh Kumar
Assistant Professor,
Department of EEE,
E.V.M College of Engineering and Technology.

Abstract:

Wind energy is an important area of operation of variable-speed generators workingunder a constant grid frequency. This paper illustrates the operation and control of one of these variable-speed wind generators, the direct driven permanent magnet synchronous generator (PMSG). This generator isconnected to the power network by means that of a totally controlled frequency converter, which consists of a pulsewidth-modulation (PWM) rectifier, associate intermediate dc circuit, and a PWM inverter. This paper presents a basic rule to design multilevel modular high power converters for large wind turbine power conversion. In this paper, high power medium voltage wind converter topology with a grid side isolation transformer is proposed.For future large wind turbines medium-voltage power conversion is usuallypreferred, in terms of reduced current level,higher power density, associated losses, and cost of the equipment used.For wind conversion we required a huge dc-link capacitor which is described as the topology of the system.

To compensate the ripple powerwe proposed a grid-side inverter of the multilevel modular converter, since dc-link capacitor necessity is decreased. The paper has validated the effectiveness of fuzzy logic controller for this purpose. In this paper the grid-side power quality will not be affected for the proposed ripple powercompensation scheme, even though there may be low-frequency harmonics in the transformer secondary windings. The proposed control algorithm under steady and dynamic load conditionsthe results obtained by simulation using Matlab/Simulink are very flexible and effective. Simulation results forthe proposed converter topology and control strategy with a 10-MW, 10-kV system under reduced dc-link voltage ripple is validated.

Key Terms:

Permanent Magnet Generators (PMG's), Integrated Gate Commutated Thyristor (IGCT),total harmonic distortion (THD), fuzzy controller, Pulse Width Modulation (PMW).

1.INTRODUCTION:

Nowadays we step forward for the renewable energy sources to make good environment, one of the main approach is to generate power by wind turbines. In the present generation we are using variable speed wind turbines of 1.5-3 MW, but the increasing demand of sustainable energy a 7 MW wind turbines are appearing recently and making steps forward generating wind turbines 10 MW and more economical [1]. We usedoubly fed induction generator based system for most of the wind turbine systems, but these type of generators have a complicated drive train structure which results in lower reliability especially for offshore applications so we usedirect-drive permanent magnet generators (PMGs) with full power converter due to simplified drive train structure and thus higher reliability.

Most of the present wind generator and power converter systems are based totally at the 690Vand two voltage-source or current source converters are typically used [3]. The wind turbine power ratings continuous increase sothat it can generate larger current, e.g., from 1673 A for 2-MW system to 8810 A for 10-MW system.To handle the increasing currentpower converters square measure so connected in parallel [5]. For the moment large current transfer leads to a parallel connection of multiple power cables taking place through the tower and causes substantial losses, voltage drop, further as high cost of cables, switch gears, and terminal connections [7].

ISSN No: 2348-4845
International Journal & Magazine of Engineering, Technology, Management and Research
A Peer Reviewed Open Access International Journal

By inserting the transformer (e.g., 690 V/33 kV) into the nacelle these disadvantages can be set off. Anyhow, the large and heavy electrical device occupies the restricted house of the nacelle and will increase the mechanical stress of the tower.For these reason, for large wind power conversion medium-voltage power conversion system (e.g., 10 kV) would be a lot of fascinating by reducing this level and associated cable cost and losses, further as rising the system power density.The benefits of appropriate medium-voltage power conversion technology are tested in motor drive applications, wherever medium-voltage (3–33 kV) configuration is mostly usedwhen the system power rating is higher than 1 MW [8]. Table I shows the current rating of associate degree ideal5- and 10-MW systems with 690-V and 10-kV voltage level for comparison. As seen, convert from low voltage (690 V) to medium voltage (10 kV) can significantly decrease the current level.

Another, considering the high maintenance cost and fault-tolerant demand particularly for offshore wind applications, a modular converter and generator structure is even desirable.With reference to medium-voltage multilevel converter topology for wind power benefits, papers [9]-[12], investigate the quality of three-level neutral-point-clamped converters. The ac-side voltage is limited to 4.0 kV if using 4.5-kV integrated gate-commutated thyristors (IGCTs) so that a better voltage rating and reduced output harmonics are achieved.The voltage rating could also be further increased if using 6-kV IGCT; but, the price and handiness becomes a serious concern.To increase the device voltage and power capabilitya five-level hybrid converter topology with increasing number of devices is used.However, the reliability restricts its application. If one device fails, the complete converter system operation would be broken.

TABLE I:Wind Turbine Current Ratings For Different Voltage Levels

Wind turbine power (MW)	voltage (kV)	Current(A)
5.0	0.69	4400
	10	303
10	0.69	8810
	10	607

Through the cascaded modular converter structureas shown in Fig. 1, we can achieve 6- or 10-kV medium-voltage power conversion is [2], [8].

Various Papers have proposed varied convertor topologies supported this idea. By cascading more converter cellsthe voltage level may be simply scaled up.However, the basic connections between these topologies don't seem to be analyzed. For fault-tolerant operation capability the cascaded convertor topology has essential.If one cell fails, it will be bypassed and also the rest healthy cells will keep operation [12]. The giant dc-link capacitor needed to filter the dc-link voltage ripple from the H-bridge side in every cell. One of the most disadvantages of the cascaded device topology [11].The dc-link capacitor is unreliable and is not favored in wind power applications wherever maintenance price is incredibly high. To considerably cut back the dc linkcapacitorthere aren't any effective solutions. In motor drive applications, diode rectifiers are normally used. Butthese cannot be actively controlled to compensate the ripple power so reducing the dc-link capacitor. In this paper, a basic rule to construct multilevel modular high power converters for large wind turbine power conversion is proposed. Using a generalized approach for an exemplar 10-kV, 10-MW wind turbine based on this, three potential multilevel modular wind power converter topologies have been derived. A special focus has been given to the topology comprising a 10-kV

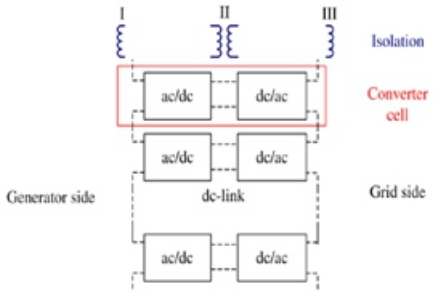

Fig.1: Generalized cascaded multilevel converter topology

A solution to cut back the dc-link capacitor is projected by compensating the ripple power from the three-phase grid-side inverter. The current harmonics induced in thetransformer secondary windings and inverter by the proposed control scheme and their impact are also investigated analytically. The converter topology and dc-link capacitor reduction strategy has been simulated and validated with a 10-kV, 10-MW wind power conversion system. The dc-link voltage ripple is effectively attenuated without affecting the grid power quality.

ISSN No: 2348-4845
International Journal & Magazine of Engineering, Technology, Management and Research
A Peer Reviewed Open Access International Journal

2. WIND ENERGY

2.1 Electricity Generation:

In generating wind energy we use a group of individual turbines which are interconnected with a medium voltage (often 34.5 kV), along with power collection system and communications network,so called a wind farm. The generated voltage is increased with a transformer so that it can be fed to the high voltage electric power transmission system. This seamlesspower is fed into the network with some limitations and sold to the utility industries, gaining a retail credit for the very small generator's owners to requite their energy costs.

As we know, wind speed is never constant, so as wind generation. Hence, the annual wind energy generation is never equal to the sum of the generator nameplate ratings multiplied by the total hours in a year.So the capacitive factor (the ratio of actual productivity in a year to the theoretical maximum) is very low i.e., 20–40%,with values at the upper end of the range especially in favorable areas. For example, a 1 MW turbine with a capacity factor(C.F) of 35% will not generate 8,760 MWh in a year (1 × 24 × 365), but only 1 × 0.35 × 24 × 365 = 3,066 MWh, averaging to 0.35 MW. For some locations the real time data is available and the C.F can be evaluated from the yearly output. Unlike the conventional generating stations like Natural gas generating stations, the C.F is restricted by inherent characteristics of wind.

However the C.F of other types of power plantare based generally on fuel cost. These plant requires less maintenance with high productivity such as Nuclear plants which have low incremental fuel cost and with a full output 90% C.F. some plants uses fuel as input so that they can operate only to follow load to meet peak power demand because of the fuel cost. A gas turbine plant may have an annual C.F of 5–25% as a result of comparatively high energy cost.

2.2 Wind Expression:

Pw is the mechanical power extracted from the airflow [W], D the air density [kg/m3], c_p the performance coefficient or power coefficient, λ the tip speed ratio Vt/Vw, (the ratio between the blade tip speed Vt and the wind speed upstream the rotor Vw [m/s]) θ the blade pitch angle [deg], and Are the area swept by the rotor [m2].

$$p_w = \frac{\rho}{2} c_p(\lambda, \theta) A_r v_w^3 \qquad (1)$$

•Cutin wind speed (in the order of 35 m/s) and
•Nominal wind speed or rated wind speed: wind speed at which the nominal power of the turbine is reached (between 11 m/s and 16 m/s).
•Cut out wind speed: When the speed of wind becomes very high, the architectural loads on the turbine become very high due to the energy content in the airflow the turbine is taken out of generation. Depending on whether the wind turbine is suitable for low or high wind speeds, (between 17 m/s and 30 m/s).
•When the speed of wind increases to levels above the normal wind speed, the load on the generator so as the converter (if present) because the generator power cannot be increased further.Hence the aerodynamic efficiency of the turbine should be minimized, in order to restrict the power generated from the wind to the normal power of the generating system.

2.3 Power from Wind:

There are mainly two factors that contribute to the efficiency of the wind turbine in generating the power from the wind. Firstly the speed of wind one of the two main factors in deciding how much energy can be generated from the wind. Because kinetic energy from the wind is used to turn the wind turbine so as the generator which in turn produces electricity.This is because the power generated from the wind turbine is a function of the cubed of the wind speed.Thus, the wind speed if doubled, the power generated will be increased by eight times the original power. Hence, the location of the wind farm plays a key role for the extraction of most available energy from the wind by the wind turbine.The design of the rotor blade is the second important factor of the wind turbine.One of the important aspects of the wind turbine is the length of the rotor blades since the power generated from the wind is also proportional to the swept area of the rotor blades i.e. the square of the diameter of the swept area.

$$P_{wind} = \frac{\Pi}{8} dD^2 v_{wind}^3 \qquad (2)$$

Hence, by doubling the diameter of the swept area, the power generated will be four fold increased. So the rotor blades would be strong, light in weight and durable. These qualities of the rotor blades become more volatile as the length of the blade increases.

ISSN No: 2348-4845
International Journal & Magazine of Engineering, Technology, Management and Research
A Peer Reviewed Open Access International Journal

So the manufacturers took advances in manufacturing the rotor blades using fiberglass and carbon fiber technology, the production of strongand lightweight rotor blades of length 20-30 meters is possible. These type of wind turbines with massive rotor blades are capable to generate up to 1 MW of power.It should be noted that some books derived the formula in terms of the swept area of the rotor blades (A) and the air density is denoted as 0¬¬. So before choosing a wind turbine one should make sure the one that can make the best use of the available kinetic energy of the wind. Wind power has the subsequent advantages over the standard power plants, Complementary generation, Rapid construction, Modular installation, Improving price competitiveness, improved system reliability and Non-polluting.

3. Grid-side inverter model and control strategy:

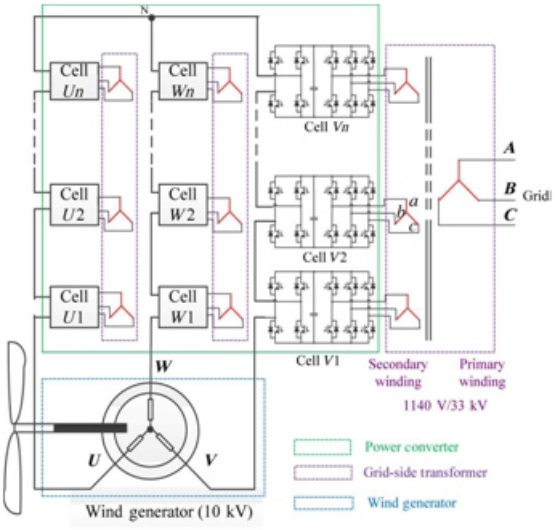

Fig. 2: High-power, medium-voltage (10 kV) modular wind converter with grid-side transformer isolation

Fig. 2Shows the high-power, medium-voltage windconverter topology with a grid-side isolation transformer, this topology adopts a standard 10-kV wind generator and a grid-side step-up transformer with multiple secondary windings (1140 V/33 kV), which provides isolation of each converter cell and also boosts the converter voltage to the grid voltage of 33 kV. The power converter and the transformer can be put at the bottom of the tower. This reduces the mechanical stress of the tower and saves the space in the nacelle. The input stage of each converter cell is an H-bridge rectifier which is thenconnected in series to achieve 10-kV voltage capability to control the generator.

The output stage of each converter cell is a three phase inverter and is connected to the transformer secondary windings.The cascaded H-bridge converter in high power motor drive area, this topology may become a strong candidate for future large wind turbine power conversion systems. It should be noted that the low-frequency single-phase fluctuating power at the input stage of each cell (H-bridge) in Fig. 2. will cause dc-link voltage ripple, which gets larger with lower generator stator frequency and higher power level. For variable speed, direct-drive PMGs, the stator frequency is generally low (e.g., below 15 Hz). Therefore, large dc-link capacitance is required to smooth out the voltage ripple appeared on the dc link, the dc-link capacitance is bulky and significantly increase the system cost as well as cause reliability issues due to the lifetime of electrolytic capacitors.The dynamic model of the grid connection when selecting are reference frame rotating synchronously with the grid voltagespace vector is[11],

$$u_d = u_{id} - Ri_d - L\frac{di_d}{dt} + \omega Li_q$$

$$u_q = u_{iq} - Ri_q - L\frac{di_q}{dt} - \omega Li_d \quad (3)$$

Where L and R are the grid inductance and resistance, respectively, and $u_{id}$and $u_{iq}$are the inverter voltage components. If the reference frame is oriented along the supply voltage, the grid voltage vector is

$$u = u_d + j0 \quad (4)$$

Then active and reactive power may be expressed as

$$P = \frac{3}{2}u_d i_d$$

$$Q = \frac{3}{2}u_d i_q \quad (5)$$

Active and reactive power control can be achieved by controlling direct and quadrature current components, respectively. The control of this converter is quite similar to that of the generator. Two control loops are used to control the active and reactive power, respectively Fig. 3.The grid-side three-phase inverter control diagram is shown in Fig. 3. The outer loop is the dc-link voltage control loop which is kept to be 1800 VThis assures that all the power coming from the rectifier is instantaneously transferred to the grid by the inverterand inner loops are d-axis and q-axis current control loops. The q-axis current can be used to provide reactive power to the grid when required subject to the current capability of the converter.

ISSN No: 2348-4845
International Journal & Magazine of Engineering, Technology, Management and Research
A Peer Reviewed Open Access International Journal

3.1 Converter DC-Link Voltage Ripple Reduction:

One particular issue with the converter topology shown in Fig. 2 is the large dc-link capacitor required in each cell to smooth the single-phase pulsating power from the H-bridge (generator) side, which can be expressed as

$$\begin{aligned} P_{q-single}(t) &= v_{o,U}(t).i_{o,U}(t) \\ &= V_{om}\cos(\omega_o t).I_{om}\cos(\omega_o t-\varphi) \\ &= \frac{V_{om}I_{om}}{2}cos\varphi + \frac{V_{om}I_{om}}{2}\cos(2\omega_o t-\varphi) \\ &= P_{avg}.cos\varphi + P_{avg}.\cos(2\varphi_o t-\varphi) \quad (6) \end{aligned}$$

Where V_{om} and $I_{om}$are the amplitudes of the generator voltage $(v_{o,U})$and current $(i_{o,U})$seen at each cell, respectively. $P_{avg}$is the average power flowing into the converter cell.$\omega o$is the generator stator frequency and φ is the generator power factor angle. As seen, the second term in (6) represents the pulsating power with the frequency of 2ωowhich causes dc-link voltage ripple. The amplitude of dc-link voltage rippleΔV can be expressed as

$$\Delta V = \frac{P_{avg}}{\omega_o.C.V_{dc}} \quad (7)$$

Where C is the dc-link capacitor and$V_{dc}$is the dc-link voltage.As seen, the dc-link voltage ripple becomes larger with lower generator frequency and higher power rating. To keep the dc-link voltage ripple with inΔV, the required dc-link capacitance C can be calculated by

$$C \geq \frac{P_{avg}}{\omega_o.\Delta V.V_{dc}} \quad (8)$$

For a 10-MW wind power converter with 15 cells (5 stages),1800-V dc-link voltage, and 15-Hz generator stator frequency,the required capacitor in each cell will be 44 mF in order to keep the voltage ripple to be within 5% (90 V) at the rated operating point.To achieve such large capacitance at this voltage level, many electrolytic capacitors need to be connected in both series and in parallel, which are not only expensive and bulky, but also cause reliability issues of the system, since the electrolytic capacitor has almost the highest failure rates in a typical wind power converter system.

For offshore applications, high reliability is a key to reduce the maintenance cost. Therefore, an effective method to reduce the required dc-link capacitor is critical. Due to the use of controlled three-phase inverter in each cell, the power transferred to the transformer secondary winding can be well adjusted to compensate the power ripple from the H-bridge rectifier.

If the power of the three-phase inverter in (5) is regulated the same as the power from the H-bridge rectifier as(6) (including the pulsating power), in theory, no dc-link capacitor is required to handle the low-frequency (2ωo) power ripple.

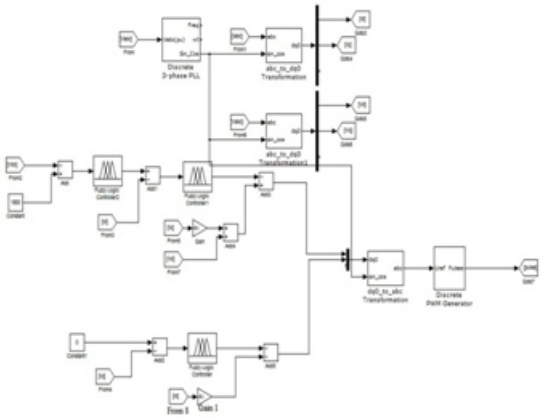

Fig. 3:Simulink block diagram of the grid-side inverter in each cell (The PI controller is replaced with fuzzy controller when the dc-link voltage ripple reduction function is enabled).

By equating (5) with (6), the inverter d-axis current becomes (9) under vector control.

$$i_{d,U} = \frac{V_{om}I_{om}}{3E}[cos\varphi + \cos(2\omega_0 t-\varphi)] \quad (9)$$

$$i_{q,U} = 0$$

Wherei_(d,U)andi_(q,U) are d-axis and q-axis currents assuming that the three-phase inverter is connected to phase U of the generator. As can be seen, the d-axis current has an AC component with the frequency of 2ω_0 , which is different from the conventional control where only dc component exists.If the d-axis current of the three-phase inverter can be controlled the same as in (9), then there will be no dc-link low frequency voltage ripple in steady state.

3.2 Current Harmonic Analysis:

In the following analysis, the generator phases are denoted by U, V, W and the transformer primary phases are denoted by A, B, C and the transformer secondary phases are denoted by a, b, c,respectively, as indicated in Fig. 2. In (9),theexpressionof d-axis current of the three-phase inverterconnecting to the cells of generator phase U is given.

ISSN No: 2348-4845
International Journal & Magazine of Engineering, Technology, Management and Research
A Peer Reviewed Open Access International Journal

Similarly,the corresponding d-axis current of the three-phase inverters ofthe cells connected to generator phases V and W can be derivedas in (10) and (11) by considering the phase shift of 120^0

$$i_{d,V} = \frac{V_{om}I_{om}}{3E}\left[cos\varphi + \cos\left(2\omega_0 t - \varphi - \frac{4\Pi}{3}\right)\right] \quad (10)$$

$$i_{d,W} = \frac{V_{om}I_{om}}{3E}\left[cos\varphi + \cos\left(2\omega_0 t - \varphi + \frac{4\Pi}{3}\right)\right] \quad (11)$$

To analyze the current harmonics in the three-phase inverter, the d, q currents given in (9), (10), and (11) are transformed back to a, b, c coordinate by using inverse-Park transformation. For the cells connecting to phaseU of the generator, the inverter phase$a$current (transformer secondary current) can be expressed as

$$i_{a,Ui} = \frac{V_{om}I_{om}}{3E}[cos\varphi + \cos(2\omega_0 t - \varphi)]\cos\left(\omega_e t + \theta_{0,Ui}\right)]$$

$$i_{a,Ui} = \frac{V_{om}I_{om}}{3E}\begin{Bmatrix} \cos(\omega_e t + \theta_{0,Ui})cos\varphi \\ +\frac{1}{2}\cos[(\omega_e + 2\omega_0)t + (\theta_{0,Ui} - \varphi)] \\ +\frac{1}{2}\cos[(\omega_e - 2\omega_0)t + (\theta_{0,Ui} - \varphi)] \end{Bmatrix} \quad (12)$$

Where$i_{a,Ui}$ represents the phase $a$current of the inverter and thesuffix U denotes the inverter cell which is connected to phase U of the generator. Suffix i denotes the i$_t$ module of the module string.$\theta_{0,Ui}$is the phase angle of the transformer secondary voltage and ω_e is the grid frequency. As seen from (12), the inverter phase current (transformer secondary current) contains not only the fundamental component with the grid frequency of, ω_e but also the frequency components of $\omega_e + 2\omega_0$and$\omega_e - 2\omega_0$. These current harmonics are due to the compensation of the power ripple from the H-bridge side. Similarly, the inverter phase $a$current of the cells connected to generator phases V and W can be expressed as in (13) and (14), respectively,

$$i_{a,Vi} = \frac{V_{om}I_{om}}{3E}\begin{Bmatrix} \cos(\omega_e t + \theta_{0,Vi})cos\varphi \\ +\frac{1}{2}\cos\left[(\omega_e + 2\omega_0)t + \left(\theta_{0,Vi} - \varphi - \frac{4\Pi}{3}\right)\right] \\ +\frac{1}{2}\cos\left[(\omega_e - 2\omega_0)t + \left(\theta_{0,Vi} - \varphi + \frac{4\Pi}{3}\right)\right] \end{Bmatrix} \quad (13)$$

$$i_{a,Wi} = \frac{V_{om}I_{om}}{3E}\begin{Bmatrix} \cos(\omega_e t + \theta_{0,Wi})cos\varphi \\ +\frac{1}{2}\cos\left[(\omega_e + 2\omega_0)t + \left(\theta_{0,Wi} - \varphi + \frac{4\Pi}{3}\right)\right] \\ +\frac{1}{2}\cos\left[(\omega_e - 2\omega_0)t + \left(\theta_{0,Wi} + \varphi - \frac{4\Pi}{3}\right)\right] \end{Bmatrix} \quad (14)$$

Where$\theta_{0,Vi}$, $\theta_{0,Wi}$ are the voltage phase angles of the transformersecondary windings of the cells connected to the generator phases V, W, respectively. In the converter and transformer configuration shown in Fig. 2, all the transformer secondary voltages have the same phase angle with respect to the primary side. Therefore, $\theta_{0,Ui} = \theta_{0,Vi} = \theta_{0,Wi} = \theta_{0.i}$.

If the inverter phase $a$currents of the cells connected to generator phases U,V, W as shown in (12)–(14), are added together, the total phase a current becomes

$$i_{a,Ui} + i_{a,Vi} + i_{a,Wi} = \frac{V_{om}I_{om}}{3E}\cos(\omega_e t + \theta_{0,Wi})\,cos\varphi. \quad (15)$$

As seen, the harmonic currents with the frequency of$\omega_e + 2\omega_0$and $\omega_e - 2\omega_0$in each cell are cancelled among the transformer secondary side. Therefore, they do not exist in the transformer primary. The transformer primary side (grid side) only contains the fundamental sinusoidal component with the frequency of ω_e. The same current harmonics analysis can be done for phases b and c. Therefore, the proposed dc-link capacitance reduction method does not affect the grid power quality.

4. Fuzzy Logic Controller:

Most of the real-world processes that require automatic control are non-linear in nature. That is, their parameter values alter as the operating point changes over time or both. As conventional control schemes as they are linear in nature, a controller can only be tuned for a limited period of time are to give good attainment at a specific operating point. From time to time, with the every change in the operating point the controller needs to be retuned. This requirement to retune has driven the demand for adaptive controllers which can match the current process characteristics by automatically retuning themselves.

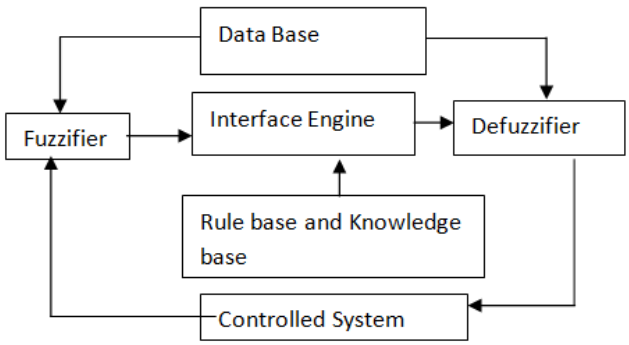

Fig. 4: Fuzzy logic controller

ISSN No: 2348-4845
International Journal & Magazine of Engineering, Technology, Management and Research
A Peer Reviewed Open Access International Journal

Fuzzy logic is an innovative technology that enhances conventional system design with engineering expertise. Using fuzzy logic, we can avoid the need for accurate mathematical modeling.The basic configuration of Fuzzy logic control based as shown in Fig. 4.Consists of four main parts i.e.

(i) Fuzzification,
(ii) Knowledge base,
(iii) Inference Engine and
(iv) Defuzzification.

4.1 Fuzzification:

Fuzzification maps from the crisp input space to fuzzy sets in certain, input universe of discourse. So for a specific input value x, it is mapped to the degree of membership A(x). The Fuzzification involves the following functions which measures the value of input variables.Assigned triangular membership functions are used as inputs and the output of the fuzzy controlleras shown in Figs. 5(a), 5(b), 5(c). Using simulations the universe of discourse for the torque error and the duty ratio is adjustedto get optimal torque ripple reduction.Since there are three membership functions for each input, it follows that there are nine rules in each set of fuzzy rules. The presented fuzzy controller is for both forward and backward rotation, for backward rotation the absolute value of the torque error is used, and the flux position calculation is adjusted according to the rotation direction.

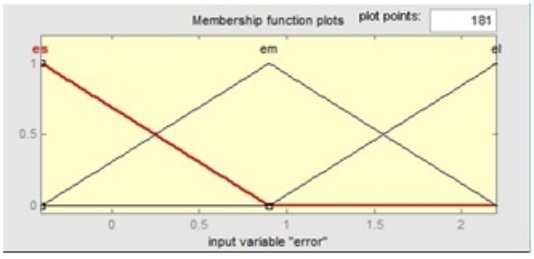

Fig. 5(a) Membership functions distribution for the torque error (input)

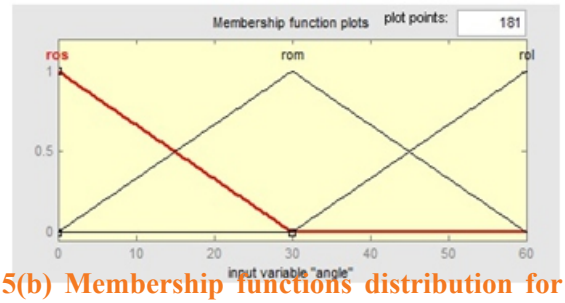

Fig. 5(b) Membership functions distribution for the torque angle(input)

If (torque error is medium) and (flux position is small) then (duty ratio is small) If (torque error is large) and (flux position is small) then (duty ratio is medium)Using the above reasoning and simulation to find the fuzzy rules, the two sets of fuzzy rules are summarized in Table II.

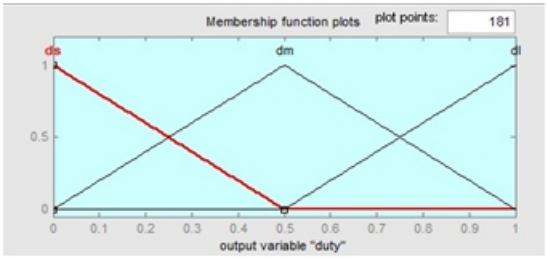

Fig. 5(c) Membership functions distribution for the duty cycle (output)

4.2 Knowledge Base:

Table IIshows rule base of the FLC.Max–Min and Max-Dot are planned within the literature of several composition methods. In the entire paper Minimum methodology is used. Knowledge base comprises of the definitions of fuzzy membership functions for the input and output variables and the required control rules, which defines the control action by using linguistic terms.

4.3 Defuzzification:

Defuzzification covers the linguistic variables to determine numerical values. Centroid method of defuzzification is used in this study.
(1)A scale mapping, this converts the range of values of input variables into corresponding universe of discourse.
(2)Defuzzification, which yields a non-fuzzy control action from an inferred fuzzy control action.

TABLE II: Fuzzy Rules

Flux Error	Torque error dt-±1 / Flux angle	Small	Medium	Large
Negative dλ=0	Small	Small	Small	Medium
	Medium	Small	Medium	Large
	Large	Small	Medium	Large
Positive dλ=1	Small	Small	Medium	Large
	Medium	Small	Medium	Large
	Large	Medium	Large	Large

ISSN No: 2348-4845
International Journal & Magazine of Engineering, Technology, Management and Research
A Peer Reviewed Open Access International Journal

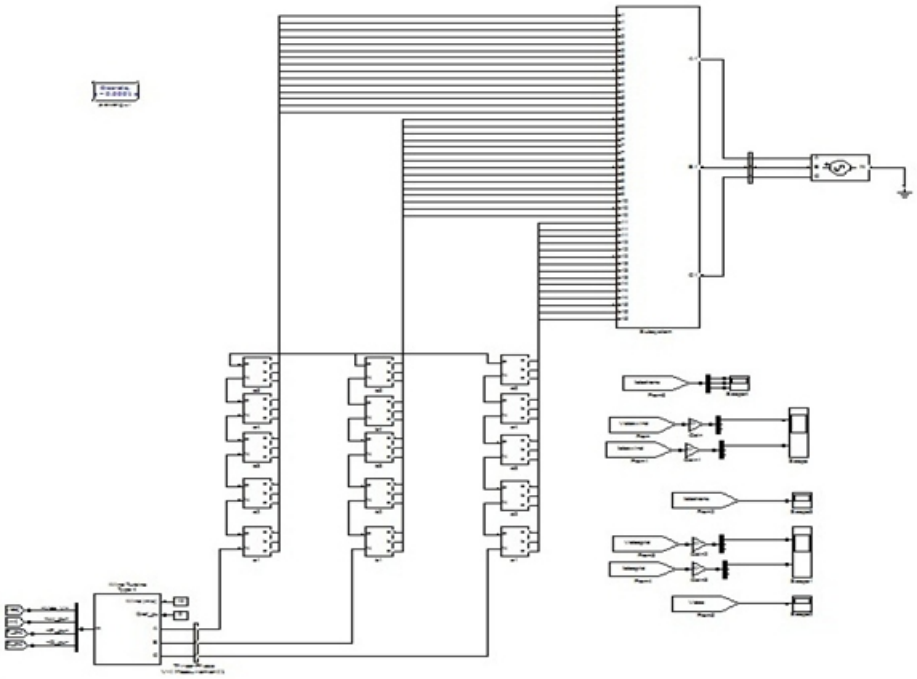

Fig. 6: Simulation model for constant wind speed by using Fuzzy Controller

5. ANALYSIS OF THE SIMULATION RESULTS:

A simulation model has been built in MATLAB/Simulink inorder to validate the converter topology in Fig. 2 and control strategy in Fig. 3. The power converter consists of 5 stages (15 cells), with each dc-link voltage of 1800 V. The dc-link capacitance is 44 mF.

A. Case 1: Steady-state simulation results at the wind speed of 12 m/s with 10-MW wind power generation.
Fig. 7(a) shows the generator-side converter output voltage,which has 11 levels and the generator current. Fig. 7(b)shows the transformer secondary winding (inverter) currents(1140-V side) in one converter cellThe grid (33 kV) phase voltage and current are shown in Fig. 7(c). As seen, the grid current is kept sinusoidal and the phase relationship between voltage and current indicates wind power is fed into the grid.

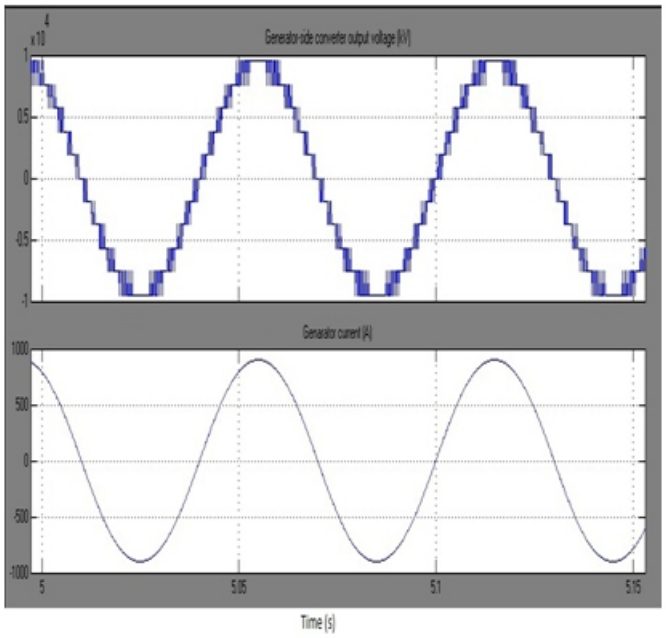

(a)

ISSN No: 2348-4845
International Journal & Magazine of Engineering, Technology, Management and Research
A Peer Reviewed Open Access International Journal

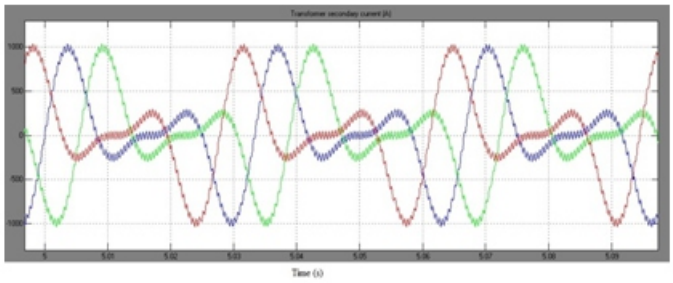

(b)

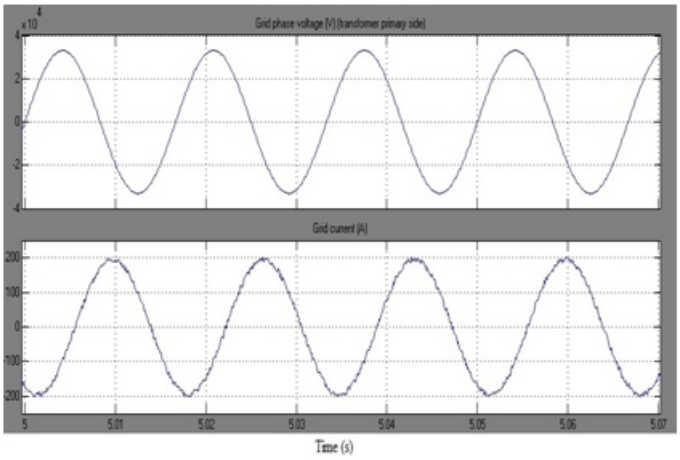

(c)

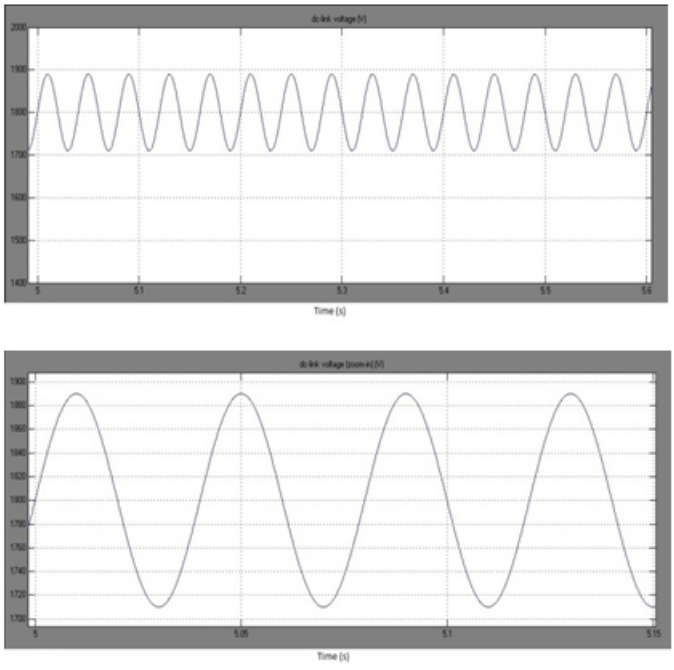

(d)

Fig. 7:Steady-state simulation results at wind speed of 12 m/s: (a) generator side converter output voltage and generator current, (b) transformer secondary winding current in a converter cell, (c) grid phase voltage and current, and (d) dc-link voltage and detailed trace.

Fig. 7(d) shows the dc-link voltage regulated at 1800 V. With 44-mF dc-link capacitor, the voltage ripple is around 90 V, which agrees with the calculated results by (7). A detailed waveform is shown at the bottom of this figure and the ripple frequency is 30 Hz, which is twice of the generator frequency of 15 Hz.

B. Case 2: System response during wind speed drop from 12 to 10 m/s.

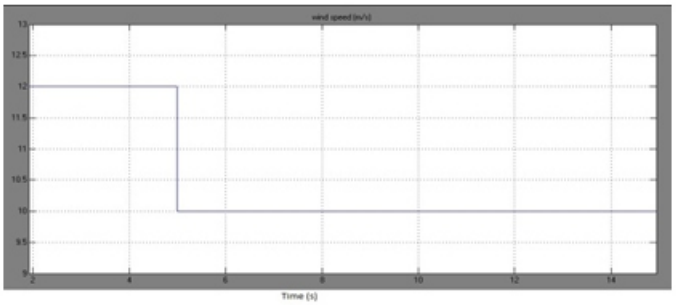

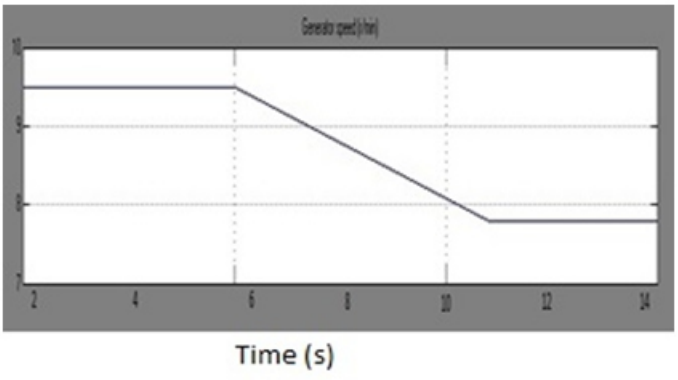

(a)

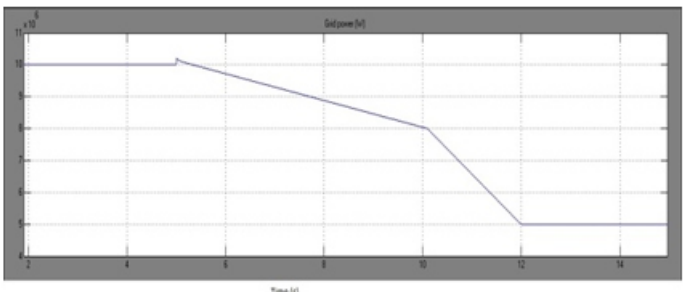

ISSN No: 2348-4845
International Journal & Magazine of Engineering, Technology, Management and Research
A Peer Reviewed Open Access International Journal

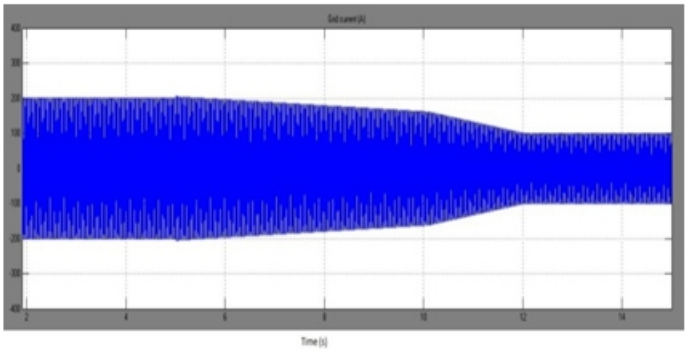

(b)

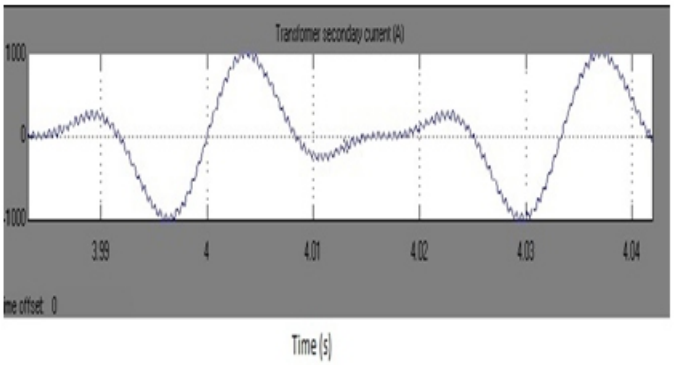

Fig. 8: System response during wind speed drop from 12 to 10 m/s: (a) wind speed and generator speed and (b) power transferred to the grid and grid current

Fig. 8 shows the system response during a wind speed drop from 12 to 10 m/s at 5 s. The converter and generator control aims to achieve MPPT under both wind speeds. Fig. 8(a) shows the wind speed profile and the corresponding generator speed. As seen, the generator speed reduces from 9.5 (MPPT point for 12 m/s) to 7.7 r/min to reach the MPPT point.Fig. 8(b) shows the power transferred to the grid and the grid current.

C. Case 3: Simulation results with a FUZZY controller:

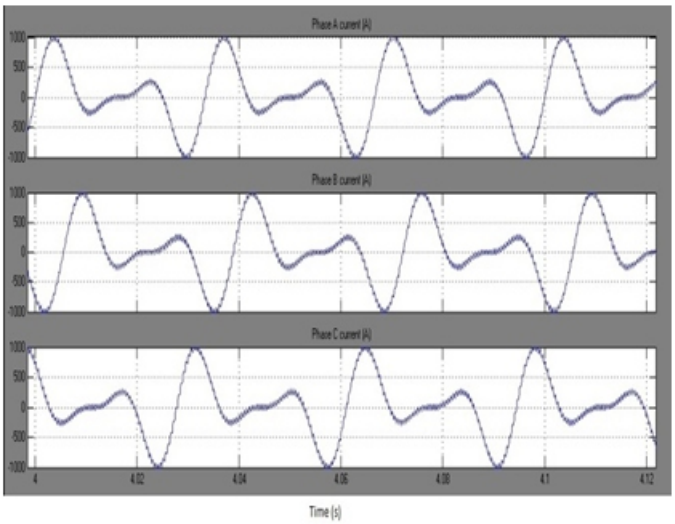

(a)

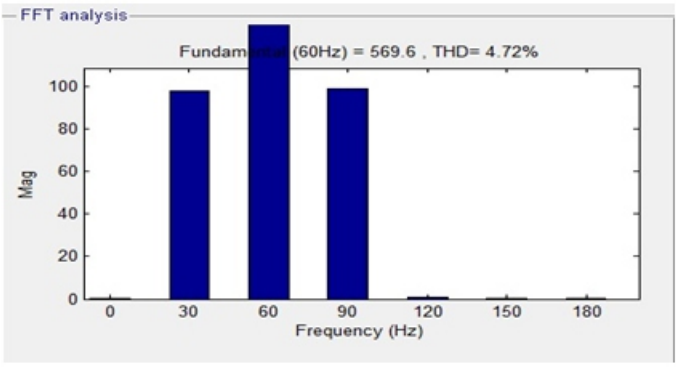

(b)

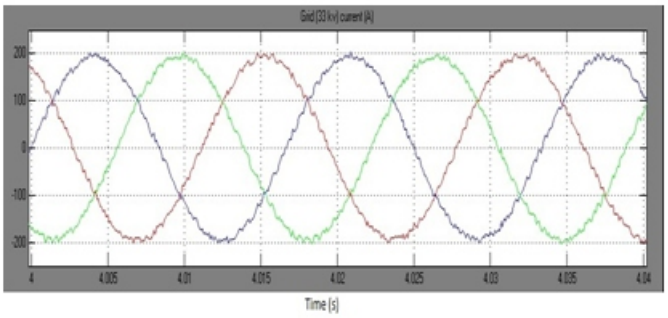

(c)

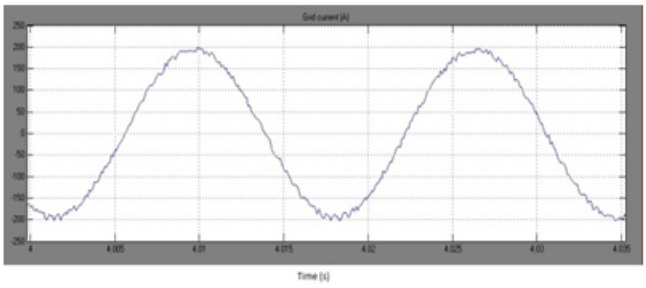

ISSN No: 2348-4845
International Journal & Magazine of Engineering, Technology, Management and Research
A Peer Reviewed Open Access International Journal

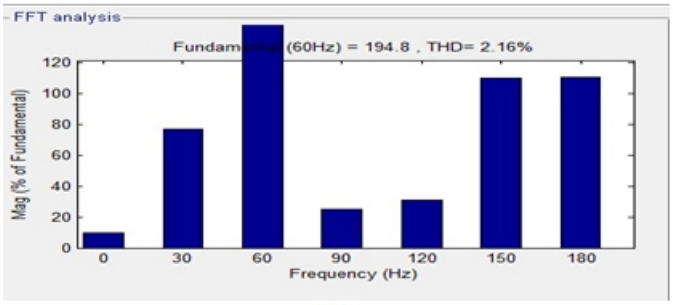

(d)

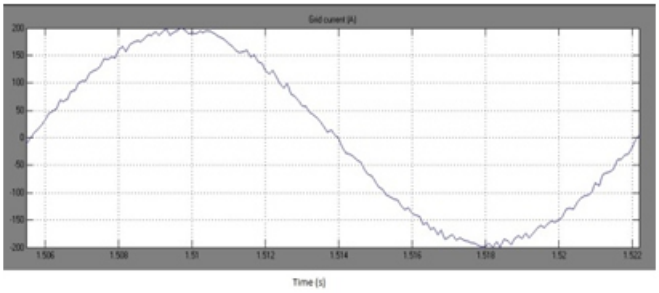

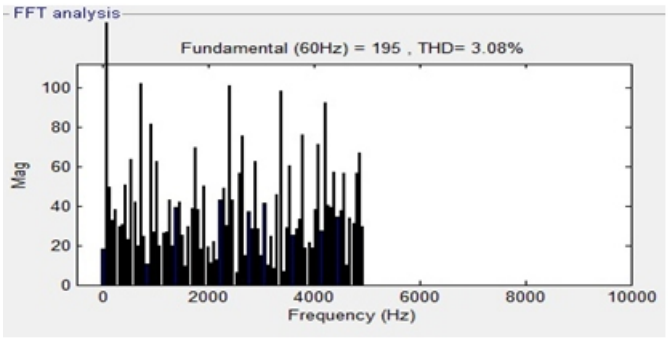

(e)

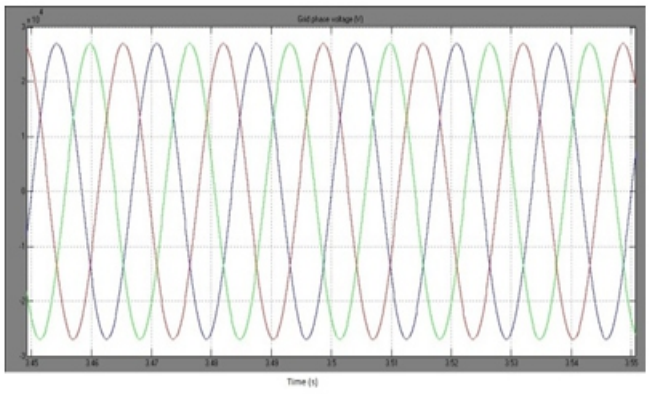

(f)

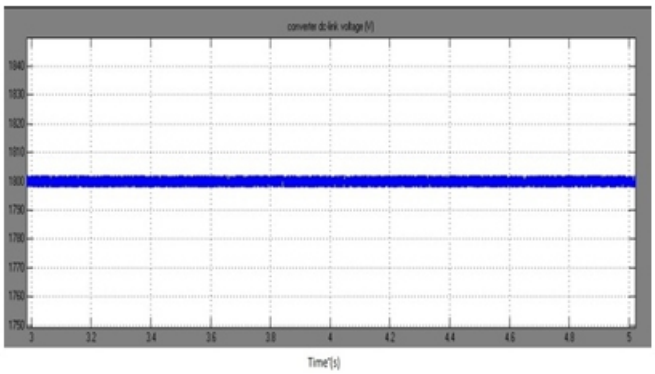

(g)

Fig. 9: Simulation results with a FUZZY controller engaged to reduce the dc-link voltage ripple (a) transformer secondary winding current, (b) FFT analysis of transformer secondary winding current, (c) transformer primary (grid) current, (d) FFT analysis of transformer primary winding current, (e) THD of the grid current, (f) grid phase voltages with phase 10% drop at 3.5 s, and (g) converter dc-link voltage under unbalanced grid.

Fig. 9 shows the results of dc-link voltage ripple reduction by using the FUZZY controller in the dc-link voltage and current control loops of each converter cell, as illustrated in the diagram in Fig. 4To observe the effect more clearly, the dc-link capacitance has been reduced from 44 to 22 mF. Fig. 9(a) shows the result ofcorresponding transformer secondary current in each cell. As seen, the currents are not sinusoidal due to the compensation of the pulsation power. As analyzed in (12)–(14), the current contains harmonics with frequency of _e+2ω_0andω_e-2ω_0.The Fast Fourier Transform (FFT) analysis of the current is shown in Fig. 9(b), where the current contains the grid-frequency (ω_e) component of 60 Hz as well as two otherfrequency components of 90 Hz (ω_e+2ω_0) and 30 Hz (ω_e-2ω_0) at the generator stator frequency (ω_0) of 15 Hz.Fig. 9(c) shows the transformer primary (grid)-side current waveform, which is sinusoidal and does not contain any low-frequency harmonics as indicated by the FFT analysis in Fig. 9(d) that only the 60-Hz grid-frequency component appears. It is evident that the proposed dc-link voltage ripple reduction method does not affect the grid-side power quality. Fig. 9(e) shows the total harmonic distortion (THD) of the grid current, which is 3.08% in this case, where the grid-interface inductance is 0.5 mHand the switching frequency is 1.95 kHz. Fig. 9(f) and (g) shows the effectiveness of the dc-link

ISSN No: 2348-4845
International Journal & Magazine of Engineering, Technology, Management and Research
A Peer Reviewed Open Access International Journal

voltage ripple reduction scheme under an unbalanced grid condition. At 3.5 s, phase Avoltage has a 10% voltage drop. From the converter dc-link voltage, it can be seen that the dc-link voltage ripple is effectively attenuated regardless the voltage drop in phase A.

6. CONCLUSIONS:

In this paper based on a generalized structure by using different formats of isolationthe high-power medium-voltage (10 kV) modular wind power converter have been derived.For reducing the capacitor requirement, by compensating the low-frequency power ripplea way has been projected to attenuate the dc-link voltage ripple, A Fuzzy controller-based control loop has been designed to achieve this purpose. The proposed dc-link voltage reduction scheme will introduce harmonics in the transformer secondary current; but, not degrading the grid power quality (sinusoidal current). Thecurrent harmonics will increasethe transformer copper loss and the stress of the power devices. Simulation results with a 10-kV, 10-MW system have validated the converter topology and control scheme.

REFERENCES:

[1]M. Liserre, R. Cardenas, M. Molinas, and J. Rodriguez,"Over viewofmultiMW wind turbines and wind parks," IEEE Trans. Ind. Electron., vol. 58, no. 4, pp. 1081–1095, Apr. 2011.

[2]F.Blaabjerg,M.Liserre,andK. Ma,"Power electronics converters forwind turbine systems," IEEE Trans. Ind. Appl., vol. 48, no. 2, pp. 708–719, Mar. 2012.

[3]M. Chinchilla, S. Arnaltes, and J. Burgos, "Control of permanent-magnet generators applied to variable-speed wind-energy systems connected to the grid,"IEEETrans.EnergyConvers.,vol.21,no.1,pp.130-135,Mar.2006.

[4]J. Dai, D. Xu, and B. Wu, "A novel control scheme for current–source– converter-based PMSG wind energy conversion systems," IEEE Trans. Power Electron., vol. 24, no. 4, pp. 963–972, Apr. 2009.

[5]J. Birk and B. Andresen, "Parallel-connected converters for optimizing efficiency, reliability and grid harmonics in a wind turbine," in Proc. EPE'07 Conf., Aalborg, Denmark, Sep. 2007, pp. 1–7.

[6]Z. Xu, R. Li, H. Zhu, D. Xu, and C. H. Zhang, "Control of parallel multiple converters for direct-drive permanent-magnet wind power generation systems," IEEE Trans. Power Electron., vol. 27, no. 3, pp. 1250–1270, Mar. 2012.

[7]W. Erdman and M. Behnke, "Low wind speed turbine project phase II: The application of medium-voltage electrical apparatus to the class of variable speed multi-megawatt low wind speed turbines," San Ramon, CA, USA, Natl. Renew. Energy Lab. Rep., NREL/SR-500-38686, Nov. 2005.

[8]H. Abu-Rub, J. Holtz, J. Rodriguez, and G. Baoming, "Medium-voltage multilevel converters-state of the art, challenges and requirements in industrial applications," IEEE Trans. Ind. Electron., vol. 57, no. 8, pp. 2581–2596, Aug. 2010.

[9]R. C. Portillo, M. M. Prats, J. I. Leon, J. A. Sanchez, J. M. Carrasco, E. Galvan et al., "Modelling strategy for back-to-back three-level converters applied to high-power wind turbines," IEEE Trans. Ind. Electron., vol. 53, no. 5, pp. 1483–1491, Oct. 2006.

[10]C. L. Xia, X. Gu, and Y. Yan, "Neutral-point potential balancing of threelevel inverters in direct-driven wind energy conversion system," IEEE Trans. Energy Convers., vol. 26, no. 1, pp. 18–29, Mar. 2011

[11]X. Yuan, J. Chai, and Y. Li, "A transformer-less high-power converter for large permanent magnet wind generator systems," IEEE Trans. Sustain. Energy, vol. 3, no. 3, pp. 318–329, Jul. 2012.

[12]M. A. Parker, C. H. Ng, and L. Ran, "Fault-tolerant control for a modular generator converter scheme for direct drive wind turbines," IEEE Trans. Ind. Electron., vol. 58, no. 1, pp. 305–315, Jan. 2011

[13]M. A. Perez, J. R. Espinoza, J. R. Rodriguez, and P. Lezana, "Regenerative medium voltage AC drive based on a multicell arrangement with reduced energy storage requirements," IEEE Trans. Ind. Electron., vol. 52, no. 1, pp. 171–180, Feb. 2005.

ISSN No: 2348-4845
International Journal & Magazine of Engineering, Technology, Management and Research
A Peer Reviewed Open Access International Journal

Author's Details:

Mr. PONNAM PRASANNAKUMAR was born in India in the year of 1991. He is pursuing M.Tech degree in Power electronics in EEE Department in EVM College of Engineering & Technology, Andhrapradesh State, India.

Mr. MAHESHKUMAR MARADUGU was born in India. He received B.Tech degree in Electrical and Electronics Engineering from Sri Chundiranganayakulu engineering college & M.Tech degree in power electronics from narasaraopet engineering college. His research interests are in the area of power systems especially generation, transmission, distribution and utilization of electrical energy.